Genome-Wide association study uncovers pea candidate genes and pathways involved in rust resistance

Salvador Osuna-Caballero*, Diego Rubiales & Nicolas Rispail

Institute for Sustainable Agriculture, CSIC, Avenida Menéndez Pidal s/n, 14004, Córdoba, Spain
* Corresponding author: Salvador Osuna-Caballero (salvador.osuna@csic.es), ORCID: 0000-0001-5325-9663

Abstract

Pea is an important temperate legume crop providing plant-based proteins for food and feed worldwide. Pea yield can be limited by a number of biotic stresses, among which, rust represents a major limiting factor. Some efforts have been made to assess the natural variation in pea resistance, but its efficient exploitation in breeding is limited since the resistance loci identified so far are scarce and their responsible gene(s) unknown. To overcome this knowledge gap, a comprehensive Genome-Wide Association Study (GWAS) on pea rust, caused by *Uromyces pisi*, has been performed to uncover genetic loci associated with resistance. Utilizing a diverse collection of 320 pea accessions, we evaluated phenotypic responses to two rust isolates using both traditional methods and advanced image-based phenotyping. We detected 95 significant trait-marker associations using a set of 26,045 DArT-seq polymorphic markers. Our *in-silico* analysis identified 62 candidate genes putatively involved in rust resistance, grouped into different functional categories such as gene expression regulation, vesicle trafficking, cell wall biosynthesis, and hormonal signalling. This research highlights the potential of GWAS to identify resistance sources, molecular markers associated with resistance and candidate genes against pea rust, offering new targets for precision breeding. By integrating our findings with current breeding programs, we can facilitate the development of pea varieties with improved resistance to rust, contributing to sustainable agricultural practices and food security. This study sets the stage for future functional genomic analyses and the application of genomic selection approaches to enhance disease resistance in peas.

Keywords

DArTseq marker, GWAS, *Pisum*, plant breeding, quantitative resistance, *Uromyces pisi*

Key message

Candidate genes and metabolic pathways controlling resistance to rust disease in pea have been proposed through GWAS using 26,045 DArTseq polymorphic markers and phenotypic data from field and controlled conditions.

1 Introduction

Pea (*Pisum sativum* L. 2n = 14) is one of the principal legume crops grown globally, ranking as the third most produced pulse in the world after dry beans (FAOSTAT 2022). This crop is a vital source of plant-based protein for both animal feed and human food, offering significant health benefits (Tulbek et al. 2016; Clemente and Olias 2017). Additionally, pea plays a crucial role in agricultural sustainability through nitrogen fixation enhancing soil fertility and structure, making it a valuable component of crop rotation or intercropping systems, particularly in conjunction with cereals (Skoufogianni et al. 2019; Gungaabayar et al. 2023).

Peas are prone to various diseases and pests, which are principal factors limiting their yield (Rubiales et al. 2015, 2023). Rust disease poses a substantial threat in many pea-growing regions worldwide. Caused by two biotrophic fungi, *Uromyces viciae-fabae* (Pers. de Bary) in warm, humid climates, and *U. pisi* (Pers.) (Wint.) in temperate zones, rust can lead to significant yield reductions—up to 50% for *U. viciae-fabae* and 30% for *U. pisi* infections (Barilli et al. 2012a; Singh et al. 2023). Such impacts on yield and seed quality underscore the necessity for focused breeding and management strategies to effectively counteract rust disease in peas..

Rust control with fungicides is effective (Emeran et al. 2011) but requires repeated treatments which is hardly economical for low input field crops like pea. Also, concerns are raised on environmental issues of pesticide control. To

address this, efforts have been made to control pea rust inducing systemic acquired resistance (Barilli et al. 2009b) or using natural compounds, that were shown promising although the available formulations are only partly effective, and their long-term environmental impacts remain unverified (Barilli et al. 2012b, 2017, 2022). Therefore, further emphasis is needed to develop cultivars resistant to rust. In this line, large pea germplasm collections have been evaluated for resistance to *U. pisi*, disclosing and characterizing variable levels of incomplete resistance, with no complete resistance available so far (Barilli et al. 2009a; Osuna-Caballero et al. 2022). Partial resistance (PR) is characterized by a non-hypersensitive response and reduced disease severity (DS). It is very frequent in other legumes against various rusts, and it is the common source of resistance found in peas against rust (Rubiales et al. 2011). Conversely, hypersensitive resistance (HR), often monogenic in origin, has also been observed in other rust pathosystems caused by *U. viciae-fabae* in lentils and faba beans (Avila et al. 2003; Negussie et al. 2012; Rubiales et al. 2013; Adhikari et al. 2021). Recent screenings of a pea core collection have uncovered new sources of PR and identified for the first time a pea accession combining HR and PR against *U. pisi* (Osuna-Caballero et al. 2022). Furthermore, new, and more efficient image-based phenotyping methods are improving the limitations of traditional breeding in this pathosystem (Olivoto et al. 2022; Osuna-Caballero et al. 2023). Nevertheless, despite previous efforts to unravel the genetic control underlying resistance to this fungal disease—where QTL responsible for resistance in *P. fulvum* were identified—clarifying the genetic architecture of HR and PR to rust caused by *U. pisi* remains necessary (Barilli et al. 2018). Furthermore, identification of candidate genes could be instrumental in foreground selection of favourable alleles.

The phenotypic information available in pea germplasm, combined with new high-throughput phenotyping systems focused on rust (Gallego-Sánchez et al. 2020; Osuna-Caballero et al. 2023), and the availability of high-quality reference pea genomes (Kreplak et al. 2019; Yang et al. 2022), enables more in-depth genomic studies (Pandey et al. 2021). Genome-wide association studies (GWAS) have emerged as a powerful approach to dissect the complex genetic underpinnings of quantitative traits within diverse plant populations. By scanning the genome for polymorphisms correlated with phenotypic variance, GWAS has facilitated the identification of both single nucleotide polymorphisms (SNPs) and DArT-seq derived markers that are intricately linked with key traits, providing candidate genes associated with traits of interest across numerous legume species (Susmitha et al. 2023). Specifically, recent GWAS in peas have been useful to identify favourable alleles for agronomic traits or disease resistance (Alemu et al. 2022; Leprévost et al. 2023), but there is still a lack of such studies for rust disease.

In the present study, we bring new sources of resistance against two *U. pisi* isolates by employing both traditional screening methods and innovative image-based methodologies across an extensive germplasm collection of 320 pea accessions, representative of global diversity. Moreover, we explored the genetic architecture of partial resistance to rust infection through GWAS, as a preliminary step towards more efficient precision breeding. To achieve this, the phenotypic response of the world collection of pea accessions inoculated with *U. pisi* was integrated with previously generated DArT-seq polymorphic markers, revealing significant associations between them. Therefore, our in-silico analysis of the genes containing or in the vicinity of the associated markers led to the discovery of previously uncharted metabolic pathways potentially implicated in rust response.

2 Material and Methods

2.1 Plant and fungal material

Plant material consisted in a diverse core collection of 320 *Pisum* accessions of worldwide origin gathered previously at Institute for Sustainable Agriculture – CSIC to ensure an extensive range of characteristics in terms of phenotype and their genetic makeup (Rispail et al. 2023). The collection includes accessions that have already demonstrated their potential for resistance to several pea diseases including rust (accessions IFPI3260, PI347352, PI347343, PI347353 and PI347389) (Barilli et al. 2009a).

To assess the resistance levels within the collection to rust disease, we used in this study two highly virulent isolates of *Uromyces pisi* that specifically affect pea crop, UpCo-01 and UpKeS-05, preserved at IAS – CSIC (Barilli et al. 2012a).

2.2 Phenotyping

Three series of experiments were conducted to assess the rust resistance components of the pea collection. One series of experiments took place under field conditions over three cropping seasons, involving adult plants, while the other two experiments were conducted in controlled conditions (CC) using seedlings infected with the *U. pisi* isolate UpCo-01 or UpKeS-05.

For the field experiment, the pea collection was evaluated over three consecutive crop seasons from 2018 to 2020 in Cordoba, Spain, as described in Osuna-Caballero et al. (2022). Briefly, ten seeds per accession were sown in 1-meter rows, spaced 0.7 meters apart, in an alpha lattice design with three replicates. Mature plants were artificially inoculated with the *U. pisi* isolate UpCo-01, and Disease Severity (DS) was assessed as the percentage of rust coverage 30 days after inoculation (dai).

The first CC experiment, involved evaluating the pea collection against the UpCo-01 isolate, followed a randomized complete block design (RCBD), and the three inoculations involving two plants per genotype were performed on pea seedlings as described in Osuna-Caballero et al. (2022). Therefore, screening was done with six replicates per accession, visually counting pustules (Infection Frequency, IF) from 7 to 13 dai allowed to estimate the Area Under Disease Progress Curve (AUDPC), the Latency Period (LP_{50}) and the Monocyclic Disease Progress rate (MDPr). Additionally, at 13 dai, DS and infection type (IT) was also visually evaluated.

The second CC experiment utilized the UpKeS-05 rust isolate and included an additional biological replicate in the three inoculations, resulting in a total of nine replicates per genotype. The inoculation procedure was identical to the previous CC experiment, ensuring consistency in how the plants were exposed to the rust. However, at 7 dai, when the rust colonies were already stablished, a detached leaflet from each plant was placed on a Petri dish with an agar-water mixture (1:10 v:v). This method, detailed in Barilli et al. (2022), was devised to preserve leaf viability, facilitating the documentation of rust progression via imaging. Subsequent analysis of daily photographs of these Petri dishes, spanning from 7 to 13 dai, was conducted using the *pliman* package in R software (Olivoto et al. 2022). This analysis aimed to quantify infection frequency (IF), disease severity (DS), and pustule size (PS, mm^2), in addition to calculating the corresponding disease progression parameters (AUDPC, LP_{50}, and MDPr) - except for PS. The use of the RGB evaluation method, as described in Osuna-Caballero et al. (2023) underpins this approach, which has been shown to achieve a high level of concordance with traditional visual evaluations. By maintaining consistency in the inoculation procedures across both CC experiments and employing an image-based evaluation method with proven reliability and comparability to visual assessments, we assert that the results from these experiments are indeed comparable.

2.3 Phenotypic data analysis

The statistical analysis of the three phenotypic data sets (field, $CC_{UpCo\text{-}01}$, and $CC_{UpKeS\text{-}05}$) was conducted using R 4.2.2 (R Core Team, 2021) and the *lme4* package (Bates et al. 2015) for mixed models. The linear model with interaction effect used to analyse the field data from multi-environment trials was applied using the genotype effect as fixed factor, while the remaining sources of variance, such as environment, environment x genotype interaction, and replicated block nested in environments, were included as random effects variables. Prior to analysis, field data set underwent an arcsine transformation to achieve normal distribution of disease severity percentages (DS), which was confirmed by checking the assumptions of residual normality and variance homogeneity. Heritability on the mean basis (H^2) was calculated following the formula from Olivoto and Lucio (2020):

$$H^2 = \frac{\hat{\sigma}_g^2}{\hat{\sigma}_g^2 + \hat{\sigma}_i^2/e + \hat{\sigma}_e^2/(eb)}$$

Where $\hat{\sigma}_g^2$, $\hat{\sigma}_i^2$, and $\hat{\sigma}_e^2$ are the genotypic, the genotype-by-environment interaction, and the residual variance, respectively; and e and b are the number of environments and blocks, respectively.

For both controlled conditions (CC) phenotypic data sets, DS was transformed with an arcsine transformation, and other parameters related to disease progression and daily resistant components (IF and PS) were transformed with a square root transformation to achieve normal distribution. The genotype effect was included as a fixed factor, and the replicate, block, and combination of genotype and replicate were treated as random effects variables in the mixed model analysis. In case of CC, the H^2 was calculated as follows:

$$H^2 = \frac{\hat{\sigma}_g^2}{\hat{\sigma}_g^2 + \hat{\sigma}_e^2/rep}$$

Where rep means the number of replicates within the experiment (Olivoto and Lucio 2020).

For the three data sets, mean separation between accessions and the overall mean was determined using Dunnett's test ($p \leq 0.05$). The distributions are presented as best linear unbiased estimations (BLUEs) obtained from the mixed model. Correlation between estimated means under controlled or field conditions was assessed using the Pearson correlation coefficient. To simplify the complexity of the 19 traits obtained, a principal component analysis (PCA) was performed using *factoextra* R package (Kassambara and Mundt 2020).

2.4 Genotyping

The process of DNA extraction, DArTseq protocol, and data analysis were previously detailed in Rispail et al. (2023). In summary, the genotyping of the pea core collection was carried out using the DArTSeq approach, as described by Barilli et al. (2018). DNA was extracted from pooled leaves of 20 seedlings per accession and subjected to high-density Pea DArTSeq 1.0 array analysis. Data cleaning was performed to remove markers with low quality or lacking polymorphism, following the recommendations of Pavan et al. (2020). As a result, 26,045 polymorphic Silico-DArT markers were retrieved. The filtered markers were then mapped onto the improved *Pisum* reference genome sequences (Kreplak et al. 2019; Yang et al. 2022).

2.5 Genome-wide association mapping

The 26,045 genome-wide DArTseq markers were used for association mapping of rust in the GWAS panel of 320 pea accessions. In this study, a single-trait GWAS was conducted using two different models: the single locus mixed linear model (MLM) and the multi-locus Bayesian information and linkage disequilibrium iteratively nested keyway (BLINK) model (Huang et al. 2019). Both models were performed within GAPIT 3.0 (Wang and Zhang 2021) and have different assumptions: the MLM model allows for the identification of individual markers associated with the trait, while the BLINK model considers multiple markers simultaneously, considering the joint effects of nearby markers. Therefore, the analysis can capture both major and minor genetic effects contributing to the rust response variation.

The Bayesian information criterion (BIC)-based model selection procedure was used to determine the optimum number of principal components (PCs) required to efficiently control for population structure of the collection. Additionally, the Astle kinship matrix was used to estimate relatedness among individuals, further accounting for potential genetic correlations (Astle and Balding 2009).

To determine significant DArTseq markers, two different threshold levels were applied. The Bonferroni corrected LOD threshold, calculated based on the number of markers (26,045), offers a more stringent criterion to minimize false positives. On the other hand, the false discovery rate (FDR) method, proposed by Storey and Tibshirani (2003), provides a less restrictive threshold, allowing for the identification of potentially interesting markers that might be missed by the Bonferroni correction. FDR limit was set for each model and trait combination to ensure less than one false positive association with the R package *qvalue* (Storey and Bass 2022).

To visualize the results, Manhattan plots were generated, displaying the -log10(p-value) for each marker along the seven chromosomes, highlighting regions where significant associations occur. Quantile-quantile (Q-Q) plots were also performed to assess the overall distribution of p-values and evaluate whether any genomic inflation or deflation occurred though the calculation of lambda (λ) using *QQperm* R package (Petrovski and Wang 2016). All models with genomic inflation (λ) below 0.8 or higher than 1.2 were not considered. Manhattan and Q-Q plots were generated using *CMplot* R package (Lilin-Yin 2023).

2.6 Candidate genes and pathways selection

To identify potential candidate genes, we scrutinized the genomic regions surrounding the significant DArTseq markers using the Cameor and ZW6 pea reference genome browsers (https://urgi.versailles.inra.fr/jbrowse/gmod_jbrowse/?data=myData/Pea/Psatv1a/data; https://www.peagdb.com/index/).

Based on the linkage disequilibrium resulted in this pea core collection described by Rispail et al. (2023), we considered genes either containing a DArTseq marker or residing within a 30 kb window from the marker as putative candidate genes.

The process of gene annotation involved associating these candidate genes with enzyme codes to investigate their metabolic pathways using the Kyoto Encyclopaedia of Genes and Genomes (KEGG). In cases where the proteins encoded by these genes were not characterized in the KEGG database, we extended our search to include orthologous sequences. For this purpose, the TAIR database was mined to identify corresponding orthologous proteins in *Arabidopsis thaliana*. This extensive annotation approach facilitated the elucidation of the potential function of each gene and the delineation of pathways relevant to resistance mechanisms against pea rust. To enrich our analysis, we integrated this genomic data with existing literature and performed comprehensive *in silico* analyses, thereby enhancing our understanding of the genetic factors contributing to rust resistance in peas.

3 Results

3.1 Descriptive statistic, variance components, and principal component analysis

In response to the UpCo-01 isolate, all genotypes exhibited rust symptoms under both controlled conditions (CC) and field conditions, showing a diverse range of trait responses (Table 1). Most accessions demonstrated moderate symptom levels, except for Infection Type (IT), where a predominant presence of well-formed pustules (IT = 4) was observed, as indicated by the skewness for IT (-1.94). The Area Under the Disease Progress Curve for Infection Frequency (AUDPC_IF) and Monocyclic Disease Progress Rate for Infection Frequency (MDPr_IF) both highlighted the disease's progression with comparably high heritabilities (H^2 = 0.77 and H^2 = 0.73, respectively). Despite this, they varied in their descriptive statistics; MDPr_IF showed closer to a normal distribution than AUDPC_IF, as inferred from their skewness. The coefficient of variation also underscored greater disparities between these traits, evident from a higher phenotypic range in AUDPC_IF (173.07) than in MDPr_IF (16.13).

A similar pattern resulted from the evaluation against UpKeS-05, with all accessions displaying rust symptoms (Table 1). In this case the accession PI273209 also displayed necrotic spots reflecting a low IT and a late-acting hypersensitive response to rust (ESM_1). AUDPC exhibited greater skewness and a broader range of values compared to MDPr. For this isolate, however, heritabilities were lower, indicating a distinct virulence pattern. The latency period was the trait with the lowest heritabilities and coefficients of variation for both isolates, not reflecting a solid genetic component behind these variations. Therefore, not considered a selectable trait for breeding perspectives in pea rust.

Table 1. Variance components, heritability and descriptive statistic by phenotypic data set and its trait.

Data set	Trait	Average	SE	Range	Skewness	CV (%)	H^2	Accuracy
$CC_{UpCo-01}$	AUDPC_IF	36.07	1.24	173.07	1.77	61.52	0.77	0.87
	DS	20.21	0.48	55.44	0.59	42.44	0.86	0.93
	IF	50.48	1.8	252.31	2.34	63.95	0.76	0.87
	IT	3.79	0.01	1.6	-1.94	6.88	0.67	0.82
	LP_{50}_IF	9.28	0.02	2.76	0.18	4.12	0.21	0.45
	MDPr_IF	11.41	0.13	16.13	0.27	20.8	0.73	0.86
$CC_{UpKeS-05}$	AUDPC_DS	21.99	1.04	148.67	2.56	85.11	0.51	0.71
	AUDPC_IF	29.95	1.23	117.4	1.83	73.89	0.5	0.7
	PS	0.1	0.01	0.23	0.34	29.62	0.44	0.66
	DS	10.86	0.2	23.62	0.96	33.27	0.51	0.72
	IF	51.28	1.81	156.09	0.94	63.17	0.49	0.7
	LP_{50}_DS	9.31	0.08	3.69	-0.95	15.07	0.24	0.49
	LP_{50}_IF	8.98	0.07	3.51	-0.79	13.65	0.11	0.33
	MDPr_DS	0.93	0.03	3.38	1.41	60.19	0.51	0.72
	MDPr_IF	13.62	0.43	44.03	0.96	56.97	0.36	0.6
$Field_{UpCo-01}$	DS2018	28.05	0.40	53.98	1.72	23.05	0.62	0.79
	DS2019	29.73	0.52	51.58	0.85	31.07	0.74	0.86
	DS2020	31.62	0.53	47.41	0.80	29.76	0.81	0.90
	DS_field	30.79	0.39	42.56	0.94	22.91	0.75	0.87

Field conditions revealed a slightly different picture (Table 1). As a result of the polycyclic evolution of the disease in the field, DS in the three field seasons were higher than in controlled conditions for the same isolate. While the three campaigns and their estimated average (DS_field) had similar mean values and ranges, the 2018 campaign displayed a lower H^2, accompanied by a pronounced positive skewness of 1.72. This suggests that most pea accessions exhibited reduced DS in 2018 campaign which is further corroborated by its lower CV% relative to the subsequent two field campaigns.

In general, the accuracy values—interpreted as the square root of H^2— consistently exceeded 0.7 for most traits, confirming the reliability of the experimental measurements. On the other hand, strong positive (> 0.50) and strong negative (< -0.50) skewness was detected for most traits confirming the need to transform raw values to achieve a normal distribution before fitting the mixed models and predicting the estimated means (BLUEs) for each trait.

The PCA biplot provides a comprehensive visual representation of the primary patterns of variability among the nineteen traits across the three datasets (Fig. 1). The first two principal components (PCs), accounted for over 50% of the total trait variability. Dim1 differentiated traits based on their influence on rust symptoms. Traits positively contributing to rust symptoms clustered on the right, while those inversely related to disease severity, such as latency periods, are positioned on the left although with a lower contribution to the variability. In contrast, Dim2 effectively delineated traits based on the rust isolate inoculated for the evaluations. Specifically, traits assessed for UpCo-01 were situated at the top of the biplot, which combine field and $CC_{UpCo\text{-}01}$, while those associated with UpKeS-05 isolate are anchored at the bottom.

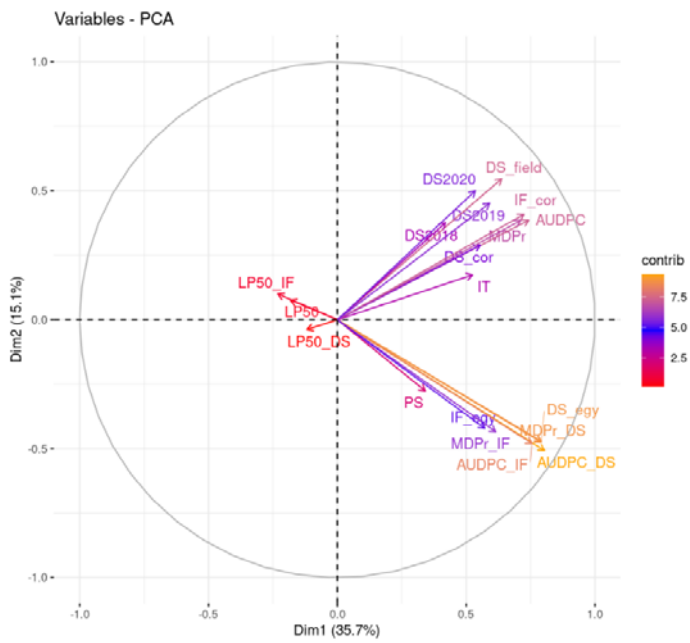

Fig. 1. PCA biplot by trait contribution to phenotypic variance.

3.2 Detection of Associated Markers

To identify genetic variations associated with rust symptoms in pea, a GWAS was conducted using two different models, MLM and BLINK, for each of the 19 traits evaluated in three conditions across 320 pea accessions. A total of 95 DArTseq markers were found to be significantly associated with some of the evaluated traits in combination with the two models applied (Fig. 2 and ESM_2). Examining the BIC estimates, the genomic inflation factor (λ) and the QQ plot revealed that population structure was efficiently controlled by the Kinship matrix without the need to add other population structure covariates (PCs) (Fig. 3, Table 2, and ESM_3).

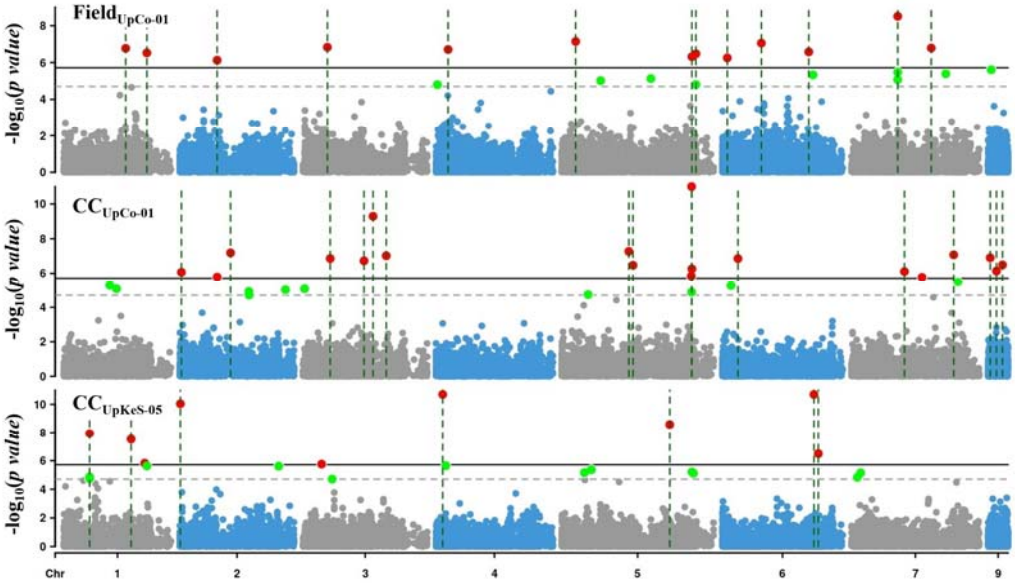

Fig. 2. Manhattan plots showing marker significance in a combination of MLM and BLINK models by phenotypic data base across pea genome. Chromosome 9 shows unmapped markers onto reference genome. Associated markers through Bonferroni-based LOD are highlighted in red and the genomic region with dashed lines while in green are the associated markers retrieved based on FDR adjustment method.

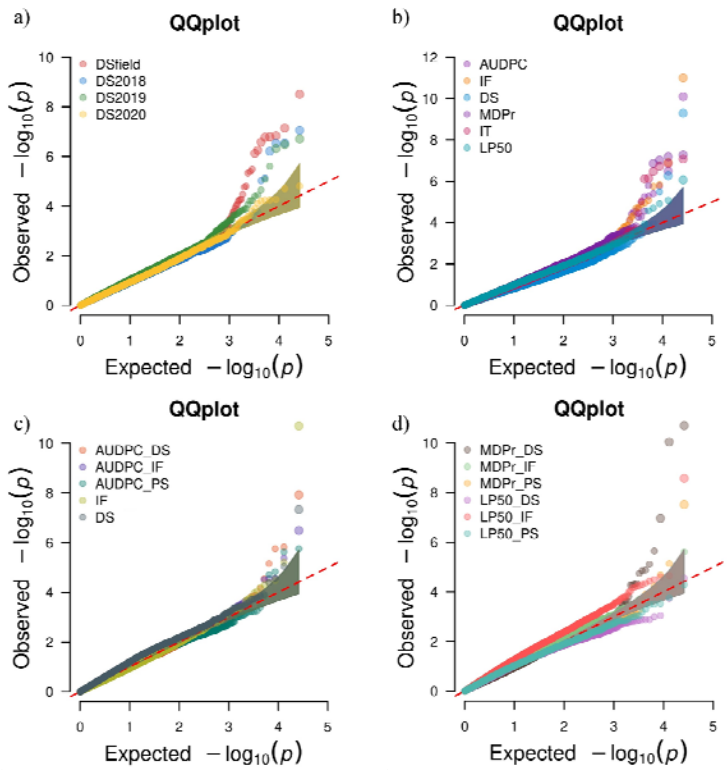

Fig. 3. Q-Q plots between theoretic and observed p values using the BLINK model. a) and b) show p values from UpCo-01 isolate in field and controlled conditions, respectively. c) and d) show p values from UpKeS-05 results in controlled conditions.

The BLINK approach identified 70 markers linked to pea rust of which 49 were unique to this model while the MLM model detected 46 associated markers of which 25 were unique to this method. Notably, 21 associated markers were common to more than one trait or model (Fig. 4a) while one marker was identified from all three data sets (Fig. 4b).

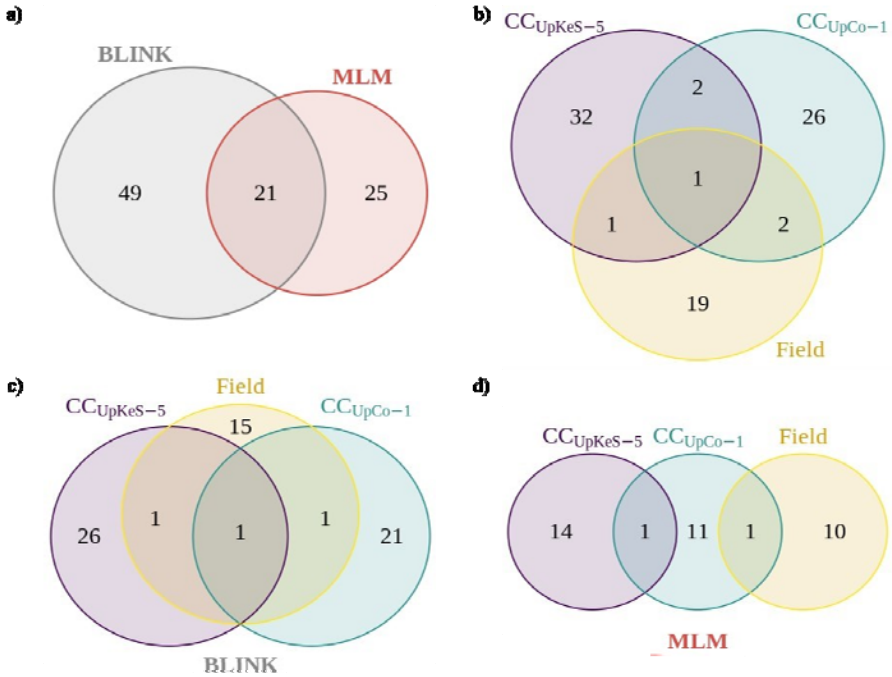

Fig. 4. Venn diagram of common markers across data sets. a) and b) represent the common associated markers by applied model and the common associated markers by phenotypic dataset in combination of both models' outputs. c) and d) show the linked markers to pea rust from BLINK and from MLM results, respectively.

In general, the BLINK model yielded a higher number of significantly associated markers with lower p-value and higher LOD (Table 2). The total phenotypic variation explained by the associated marker for each trait (PVE) varied also greatly depending on the GWAS model. As the BLINK model identified more significant marker-trait associations for each trait, their corresponding PVE_{sum} was generally higher (Table 2). The highest number of associated markers for a single trait was identified with the BLINK method for DS_field, with a total of 13 markers explaining 86.2% of the total phenotypic variance while the MLM model only uncover 3 associated markers for this trait accounting for 10.2% of the phenotypic variance (Table 2). By contrast, the MLM method uncovered 7 markers associated with AUDPC for $CC_{UpCo-01}$ while BLINK only uncovered 5 significantly associated marker for this trait although associated markers identified by both methods explained around 70% of PVE_{sum}.

Table 2. BLINK and MLM model outputs obtained for each trait from the three phenotypic data sets. N indicates the number of significant marker-trait associations; λ is the genomic inflation factor; the LOD_{range} is the range of the $-\log_{10}$(p-value); PVE_{range} is the range of the phenotypic variance explained by each individual marker and PVE_{sum} is the total phenotypic variance explained by the associated markers.

		BLINK MODEL					MLM MODEL				
Data Set	**Trait**	**N**	**λ**	**LOD_{range}**	**PVE_{range}**	**PVE_{sum}**	**N**	**λ**	**LOD_{range}**	**PVE_{range}**	**PVE_{sum}**
$CC_{UpCo-01}$	AUDPC	5	0.9	5.1-10.1	3.4-17.8	69.2	7	1.1	5.3-7.1	2.5-16.1	73.7
	DS	3	0.8	6.0-9.3	7.5-10.5	26.6	1	1.0	4.6	6.1	6.1
	IF	3	0.9	5.4-13.0	1.5-8.4	47.6	7	1.0	5.5-6.2	6.0-17.5	78.5
	IT	7	0.9	5.8-7.2	2.2-16.1	73.6	2	1.1	4.5-6.3	2.2-9.6	11.7
	LP_{50}	3	1.0	4.4-6.1	6.1-7.6	20.1	1	1.0	4.7	6.3	6.3
	MDPr	5	1.0	6.5-7.5	3.0-15.4	52.9	2	1.1	4.7-4.7	3.9-6.2	10.1
$CC_{UpKeS-05}$	AUDPC_DS	4	1.0	4.6-7.9	2.6-10.6	24.3	3	1.0	4.5-5.3	2.6-5.2	13.1
	AUDPC_IF	5	1.1	4.6-6.5	3.6-10.5	39.7	2	1.0	4.4-4.4	2.8-3.6	6.3
	PS	2	1.0	5.8-6.2	3.2-5.0	8.1	2	1.0	5.0-5.0	6.3-12.0	18.3
	DS	3	1.1	4.8-7.4	4.4-14.4	29.6	2	1.0	5.0-5.3	6.9-12.8	19.7
	IF	3	1.0	5.2-10.7	14.1-17.6	17.6	1	0.9	4.5	2.2	2.2
	LP_{50}_DS	1	1.0	4.4	5.3	5.3	1	1.0	4.5	5.3	5.3
	LP_{50}_IF	7	1.2	4.9-8.7	0.4-7.6	19.6	2	1.0	4.8-4.8	4.5-6.3	10.8
	MDPr_DS	6	0.9	5.1-10.7	3.8-15.3	58.5	6	1.0	5.3-5.9	2.5-15.3	56.1
	MDPr_IF	3	1.1	4.5-5.7	1.1-7.5	13.8	2	1.0	4.4-4.4	5.2-7.5	12.7
$Field_{UpCo-01}$	DS_field	13	1.0	5.5-8.5	0.3-14.5	86.2	3	1.0	5.1-5.4	0.5-6.8	10.2
	DS2018	5	0.9	6.3-7.0	4.6-10.2	36.5	4	1.0	5.6-6.5	4.9-10.2	29.7
	DS2019	6	1.0	5.2-7.6	1.1-22.8	77.4	6	1.0	4.7-5.5	3.5-19.5	67.7
	DS2020	2	1.0	4.6-5.0	2.9-3.1	5.9	1	0.9	4.4	1.4	1.4

It is worth noting that the sum of the phenotypic variation explained by the associated markers for each trait was closely related to heritability for the BLINK model (ESM_4), except for DS2020.

3.3 *In silico* identification of candidate genes

To identify putative candidate genes the genomic regions surrounding the significantly associated markers was examined. Out of the 95 associated markers detected (ESM_2), 75 markers were located within or next to 62 genes from the Cameor and/or ZW6 reference genomes, referred in Table 3 by their NCBI gene ID codes. It is interesting to note several of these candidate genes contained more than one significant associated marker, underscoring their importance in contributing to the phenotypic variation of the trait. By chromosome, the gene annotation results were as follows:

A total of 10 candidate genes were detected on chromosome 1. Among them, two genes, 127087512 and 127115771, each marked by two associated markers were related to vesicle trafficking within cells. Two additional genes 127115471 and 127137201 were related with wax and cell wall biosynthesis. Interestingly, one uncharacterized gene, marked by three associated markers, was related to BFA1 assembly which is required for ATP synthesis in *A. thaliana*.

On chromosome 2, 7 candidate genes were detected. Four of these genes (127120834, 127121528, 127118910 and 127117580) are related with carbohydrate and amino acid metabolism. Two genes, 127117481 encoding an F-box protein, and 127118667 encoding a MADS-box transcription factor were related to defence response to stresses in plants (Table 3) while the last identified candidate genes engaged in cell trafficking.

On chromosome 3, 9 candidate genes were detected. Among them, two genes, 127132076 and 127127305, encoded protein kinases related to plant development, stress responses and hormone signalling. Two genes, 127130208 and 127127894, were also associated with vesicle trafficking. Additionally, two genes were related with secondary metabolism while another one was related to auxin homeostasis as gene 127080599 from chromosome 1.

From the three genes detected on chromosome 4, two genes (127138368 and 127076644) encoded proteins related with the secondary metabolism and cell wall biosynthesis while the last one, gene 127138740 putatively encodes a haloacid dehalogenase-like hydrolase (HAD).

Chromosome 5 harboured the highest number of candidate gene with 18 genes identified from 23 associated markers. A notable hotspot in chromosome 5 consisted of three closely spaced markers within a 1.2 Mb window, located within genes 127082537, 127087291, and 127087323. Interestingly, two of these genes 127082537 and 127087323 were related with mobile elements in *A. thaliana* while the third one together with genes 127087766 and 127084564 were related with DNA transcription regulation. As in chromosomes 1 and 4, several genes related with cell wall biosynthesis and maintenance were detected on chromosome 5. Several genes related with transport and signalling, and with fatty acid or secondary metabolism were also detected on this chromosome.

From the five candidate genes identified on chromosome 6, three were related with DNA formation and transcription. The last two genes were related to inositol phosphate metabolism and abscisic acid (ABA) signalling, respectively.

Chromosome 7 harbour 11 genes in the vicinity of 13 associated markers. Among them, the function of three genes were not known in peas but the ortholog of two of them, 127105234 and 127105763, in *A. thaliana* have been related to tissue development. Similarly, to the other chromosomes, several candidate genes related with the regulation of DNA transcription regulation (127108155 and 127105708), the amino acid metabolism (127103253), the vesicle trafficking (127102730) and the response to stresses (127105022, 127104606 and 127104295) were identified in this chromosome.

Table 3. Potential candidate genes containing or in the vicinity of significant markers.

Gene ID_{NCBI} ■	Gene description	Pathway	DArT ID	Position ZW6†	LD	Data Set
127087512	Coatomer subunit beta'-2 in COPI	Vesicle trafficking: from Golgi to ER	3536217	Chr1_638769913	in	$CC_{UpKeS-05}$
			5922176	Chr1_638767256	in	$CC_{UpKeS-05}$
127115471	Cytochrome P450 86B1	Cutin, suberin and wax biosynthesis	3540396	Chr1_96490148	0.23 kb	$CC_{UpKeS-05}$
127121867	Uncharacterized protein	Assembly of BFA1*	41128912	Chr1_128396385	in	$CC_{UpKeS-05}$
			5916127	Chr1_128396397	in	$CC_{UpKeS-05}$
			5933458	Chr1_128395696	in	$CC_{UpKeS-05}$
127101876	Uncharacterized protein	Unknown function*	5944598	Chr1_249806845	11.83 kb	$CC_{UpKeS-05}$
			3542029	Chr1_249828952	3.94 kb	$CC_{UpCo-01}$
127135829	Guanine nucleotide-binding protein	Signal transmission outside the cell	3551012	Chr1_346012159	6.01 kb	$Field_{UpCo-01}$
127137201	Glycosyltransferase BC10	Cell wall biosynthesis*	19178657	Chr1_368992937	in	$CC_{UpKeS-05}$
127115771	Putative clathrin assembly protein	Vesicle trafficking: Clathrin-mediated endocytosis	5886489	Chr1_367783858	0.37	$Field_{UpCo-01}$
			19788813	Chr1_335454587	31.2 kb	$CC_{UpCo-01}$
127080599	WAT1-related protein	Auxin homoeostasis	3568148	Chr1_435743430	in	$CC_{UpKeS-05}$
127082329	Splicing factor 3B subunit 2	Spliceosome	26138450	Chr1_446396667	in	$CC_{UpKeS-05}$ and $Field_{UpCo-01}$
127085672	Potassium channel AKT2/3	Regulation of membrane potential, Response to abscisic acid	5926320	Chr1_461368879	in	$Field_{UpCo-01}$
127117481	F-box/kelch-repeat protein	Negative regulation of defence response	3551269	Chr2_2285562	7.45 kb	$CC_{UpKeS-05}$
127117580	Nicotinamide/nicotinic acid mononucleotide adenylyltransferase	Nicotinate and nicotinamide metabolism Metabolic pathways Biosynthesis of cofactors	5943946	Chr2_8124874	in	$CC_{UpCo-01}$
127118910	Aminoacylase	Arginine biosynthesis Metabolic pathways Biosynthesis of secondary metabolites 2-Oxocarboxylic acid metabolism Biosynthesis of amino acids	3544074	Chr2_207090849	in	$CC_{UpKeS-05}$
127118667	MADS-box protein AGL24-like	Transcription factor	3545236	Chr2_160200620	in	$Field_{UpCo-01}$
			8174445	Chr2_160210451	in	$CC_{UpCo-01}$
127103325	Uncharacterized GPI-anchored protein	Vesicle trafficking	3557565	Chr2_293250588	in	$CC_{UpCo-01}$
127120834	Hexokinase	Sugars metabolism Starch and sucrose metabolism Amino sugar and nucleotide sugar metabolism Metabolic pathways Biosynthesis of secondary metabolites Carbon metabolism Biosynthesis of nucleotide sugars	4660875	Chr2_488496120	18.91 kb	$CC_{UpKeS-05}$
127121528	Pectate lyase	Pentose and glucuronate interconversions Metabolic pathways	3557551	Chr2_453678844	6.68 kb	$CC_{UpCo-01}$
127132076	CDPK-related kinase 3	Plant development, stress responses and hormone signalling	3544108	Chr3_7935806	in	$CC_{UpKeS-05}$ and $CC_{UpCo-01}$
127125898	WAT1-related protein	Auxin homoeostasis	5937399	Chr3_149104224	in	$Field_{UpCo-01}$
127130208	Plasmodesmata-located protein	Intercellular transport	5880972	Chr3_160776867	in	$CC_{UpCo-01}$

127126068	Transcription factor EMB1444-like	Regulation of DNA transcription	4660018	Chr3_172692251	in	$CC_{UpKeS-05}$
127126145	ATP-dependent RNA helicase DHX8/PRP22	Spliceosome	4659692	Chr3_185293539	6.59 kb	$CC_{UpKeS-05}$
127127305	Serine/threonine-protein kinase PBL18	Plant development, stress responses and hormone signalling	3544804	Chr3_307444551	in	$CC_{UpKeS-05}$
127127564	Fructose-1,6-bisphosphatase, chloroplastic	Glycolysis / Gluconeogenesis Pentose phosphate pathway Fructose and mannose metabolism Carbon fixation in photosynthetic organisms Metabolic pathways Biosynthesis of secondary metabolites Carbon metabolism	3552072	Chr3_344541908	in	$CC_{UpCo-01}$
127127894	Phragmoplastin DRP1E	Defence response to fungus and vesicle-mediated transport	3555519	Chr3_390153145	in	$CC_{UpCo-01}$
127133145	Small nucleolar RNA R71		5916636	Chr3_458654213	20.98 kb	$CC_{UpCo-01}$
127138368	Peroxidase 42	Phenylpropanoid biosynthesis Metabolic pathways Biosynthesis of secondary metabolites	3559464	Chr4_10427626	22.00 kb	$Field_{UpCo-01}$
127138740	Uncharacterized protein	Haloacid dehalogenase-like hydrolase	4659565	Chr4_41816686	in	$CC_{UpKeS-05}$
127076644	Aldehyde decarbonylase	Cutin, suberine and wax biosynthesis Biosynthesis of secondary metabolites	3551373	Chr4_493077319	in	$Field_{UpCo-01}$
127087766	Chromodomain-helicase-DNA-binding protein	ATP-dependent chromatin remodelling	3538596	Chr5_90360668	in	$Field_{UpCo-01}$
127087924	ATP-dependent zinc metalloprotease FTSH 4	Proteolysis and meristem maintenance*	5934956	Chr5_99840368	in	$CC_{UpKeS-05}$
127079825	Uncharacterized protein	Unknown function*	3569894	Chr5_156765071	in	$CC_{UpCo-01}$
127080906	Uncharacterized protein	Unknown function*	3556574	Chr5_169393625	0.09 kb	$CC_{UpKeS-05}$
127082843	Long-chain acyl-CoA synthetase	Metabolic pathways Fatty acid metabolism Peroxisome	5941026	Chr5_201861329	21.33 kb	$Field_{UpCo-01}$
			5958686	Chr5_201824241	9.87 kb	$Field_{UpCo-01}$
127082981	Pectic arabinogalactan synthesis-related protein	Cell wall pectin biosynthetic process*	3567360	Chr5_211456207	in	$Field_{UpCo-01}$
127084018	Trichome birefringence-like protein	Plant-type secondary cell wall biogenesis*	3541671	Chr5_293235930	0.10 kb	$CC_{UpCo-01}$
127084160	Uncharacterized protein	Intracellular signal transduction*	3566561	Chr5_305106410	in	$CC_{UpKeS-05}$
127084564	Zinc finger CCCH domain-containing protein	Regulation of DNA transcription and translation*	3558891	Chr5_346387511	in	$CC_{UpCo-01}$
127084634	Alpha-glucan phosphorylase, H isozyme	Starch and sucrose metabolism Metabolic pathways Biosynthesis of secondary metabolites	19230512	Chr5_354090893	in	$CC_{UpKeS-05}$
127084730	4-coumarate--CoA ligase	Ubiquinone and other terpenoid-quinone biosynthesis Phenylpropanoid biosynthesis Metabolic pathways Biosynthesis of secondary metabolites	5897640	Chr5_364545534	in	$CC_{UpCo-01}$
127086095	Actin-related protein 8	Actin filament-based process*	41124830	Chr5_528086379	in	$CC_{UpKeS-05}$
127087180	Dolichol-phosphate mannosyltransferase	N-Glycan biosynthesis Metabolic pathways	5948001	Chr5_621702676	in	$CC_{UpKeS-05}$
127082537	Uncharacterized protein	Plant mobile domain*	3552142	Chr5_627629549	in	$CC_{UpCo-01}$
127087291	NLP9-like protein	Regulation of DNA-templated transcription*	3551119	Chr5_627951949	in	$CC_{UpCo-01}$
127087323	Plant transposase	Plant mobile domain*	8175311	Chr5_628892227	in	$CC_{UpCo-01}$,

						$CC_{UpKeS-05}$ and $Field_{UpCo-01}$
127087508	Sulphate transporter 3	Phosphate ion transport*	4656208	Chr5_638399837	in	$CC_{UpKeS-05}$
127096746	Chromodomain-helicase-DNA-binding	ATP-dependent chromatin remodelling	3540395	Chr6_26605159	in	$Field_{UpCo-01}$
127097832	Rho-N domain-containing protein, chloroplastic	DNA-templated transcription termination*	3557403	Chr6_68402207	in	$CC_{UpCo-01}$
127096589	Inositol polyphosphate 5-phosphatase 4	Inositol phosphate metabolism	3540217	Chr6_82691906	in	$CC_{UpCo-01}$
127091595	Retarded root growth-like protein	Involved in ABI4-mediated mitochondrial retrograde signalling*	3543069	Chr6_167359798	in	$Field_{UpCo-01}$
127097692	Guanylate kinase 1-like	Nucleotide metabolism	3535374	Chr6_449699858	in	$CC_{UpKeS-05}$
127105022	Phosphatase 1 regulatory subunit 7 protein	Abscisic acid-activated signalling pathway	3543068	Chr7_27387876	in	$CC_{UpKeS-05}$
127101904	Uncharacterized protein		5941166	Chr7_39362330	27.69 kb	$CC_{UpKeS-05}$
127103253	Amidase	Arginine and proline metabolism Phenylalanine metabolism Tryptophan metabolism Metabolic pathways	3556244	Chr7_131668232	in	$CC_{UpKeS-05}$
127108155	Cell division cycle-associated protein 7	Regulation of DNA-templated transcription	3549271	Chr7_207690490	in	$Field_{UpCo-01}$
			3541979	Chr7_207717206	26.66 kb	$Field_{UpCo-01}$
			4662232	Chr7_207717206	26.66 kb	$Field_{UpCo-01}$
127105708	Cyclic dof factor 3-like isoform X1	Regulation of DNA-templated transcription*	5900633	Chr7_237959555	in	$CC_{UpCo-01}$
127102730	Transport protein SEC31 (COPII)	Protein processing in endoplasmic reticulum, cell wall formation	3553784	Chr7_403662597	0.386 kb	$CC_{UpCo-01}$
127105234	Uncharacterized protein	Root and shoot system development*	5963353	Chr7_286715392	in	$Field_{UpCo-01}$
127105763	Uncharacterized protein	Root and tissue development*	3569870	Chr7_302256784	in	$CC_{UpCo-01}$
127104295	Secreted RxLR effector protein 161-like	Defence response (CRK8)*	3641999	Chr7_448189894	8.27 kb	$Field_{UpCo-01}$
127104606	Uncharacterized protein	Response to ABA and defence response*	3555097	Chr7_486340934	in	$CC_{UpCo-01}$
127105963	Queuine tRNA-ribosyltransferase subunit	tRNA modification factors	3562429	Chr7_506822033	in	$CC_{UpCo-01}$

▪ NCBI genes data base is in https://www.ncbi.nlm.nih.gov/gene/?term=geneID.

* Function annotation deduced from the role of its closest orthologous protein in A. thaliana.

† Physical position on the ZW6 genome of the markers, including chromosome and pb distance.

4 Discussion

Rust is a world-wide distributed disease that severely affects pea crop yield (Rubiales et al. 2015). In warm and humid areas, the main causative pathogen is *Uromyces viciae-fabae*, while *U. pisi* is responsible for pea rust in more temperate regions (Singh et al. 2023). Complete resistance to rust in peas has not yet been identified, with partial resistance being the primary source of genetic resistance available so far to control this disease in pea (Barilli et al. 2014). In this study, we applied a GWAS approach to identify regions of the pea genome associated with traits linked to the partial resistance response. To achieve this, a collection of 320 pea accessions was evaluated under field and control conditions in response to two rust isolates (UpCo-01 and UpKeS-05).

4.1 Phenotypic variance and GWAS model outputs

The evaluation method and phenotypic response of the collection against the rust isolate UpCo-01 was previously described in Osuna-Caballero et al. (2022). Here, we describe the phenotypic response of the same collection against the rust isolate UpKeS-05 obtained using the methodology described in Osuna-Caballero et al. (2023). While the seedlings inoculation followed the same procedure, this evaluation performed by images using the R software for the UpKeS-05 isolate in detached pea leaflet revealed a concordance correlation coefficient between the visual evaluation of 0.962 according to Osuna-Caballero et al. (2023). Therefore, in this study the effect of the isolates can be compared despite having obtained the phenotypic data in two different ways: an evaluation by visual counting (Osuna-Caballero et al. 2022) and another evaluation based on images using R software (Osuna-Caballero et al. 2023). These results comparison revealed some commonalities and differences. Similarly, to the situation with UpCo-01, complete resistance to UpKeS-05 was not detected in the collection. In addition, the reduced number of well-developed pustules and low IT detected on the accession PI273209 in response to UpKeS-05 suggest that this accession also exhibits a late hypersensitive resistance response against this isolate (ESM_1). Disease ratings were nonetheless lower in response to UpKeS-05 than to UpCo-01 and the response to each isolate were clearly differentiated on the PCA suggesting that the collection responded differentially to the isolates. As mild to moderate relationship was also observed for most traits between isolates, these differences are more likely revealing differences in the overall virulence level of the isolates although the existence of *U. pisi* races in peas could not be ruled out.

Previous studies performed on the pea core collection demonstrated a rapid LD decay and a broad distribution of the polymorphic DArT markers throughout the pea genome (Rispail et al. 2023). Although a significant portion of the population resulted admixed in phylogenetic terms, the collection was found to be structured into six groups consistent with the taxonomy of the *Pisum* species and subspecies (Rispail et al. 2023). However, BIC selection models indicated that population structure was efficiently controlled in the GWAS models by the kinship matrix alone and did not require adding the initial PCs to the models (ESM_3). This was previously demonstrated on GWAS studies performed on plant populations with a high percentage of admixture (Kaur et al. 2023). The BLINK model improves the statistical power and enhances the robustness of association signals compared to MLM (Huang et al., 2019). Furthermore, the extensive coverage of the DArT markers across the pea genome is ideal for multi-locus methods like BLINK, making it a frequently used model in GWAS studies to analyse complex traits in legumes (Tibbs Cortes et al. 2021; Susmitha et al. 2023). Accordingly, this method detected a high number of markers associated with rust disease development.

The two GWAS models applied here detected a total of 95 markers significantly associated with one or more of the 19 rust disease traits, among which 21 markers were detected by both methods which will be instrumental for future breeding for rust resistance in pea. The current genetic sources of pea resistance against *U. pisi* are described in the work of Barilli et al. (2010,2018). Three QTLs have been described to date. The Up1 QTL identified in linkage group 3 (chromosome 5) by Barilli et al. 2010 explained a total phenotypic variance of 63% in the biparental F_2 population between *P. fulvum* (resistant) and *P. sativum* (susceptible). These results have not been corroborated in this work, where the markers on chromosome 5 are not close to the RAPD markers that flank the QTL Up1: $OPY11_{1316}$ and $OPV17_{1078}$. The subsequent results of Barilli et al. 2018 also did not corroborate Up1 but two new QTLs UpDSII and UpDSIV were identified in linkage groups 2 and 4, corresponding to chromosomes 6 and 4, respectively. The QTL UpDSII explained an average of 24% of the phenotypic variation in the field and 28% under controlled conditions. Similarly to our results, the markers found around UpDSII revealed 16% phenotypic variation in the field and 20% for the same UpCo-01

isolate. On the other hand, the QTL UpDSIV explained 20% of the phenotypic variation both in the field and under controlled conditions according to the results of Barilli et al. (2018). Markers colocalized near UpDSIV in this work revealed an explained phenotypic variation of 26% in the field. However, no markers associated with the severity of rust caused by *U.pisi* (UpCo-01) were found on chromosome 4. These discrepancies may be due to the origin of the biparental population, due to interspecific crossing between *P. fulvum* and *P. sativum*, in counterpart of the GWAS population carrying greater genetic diversity. On the other hand, this is the first GWAS targeting rust resistance in pea while similar studies addressing rust disease in legumes remains scarce. Most previous studies were based on the MLM method while only one study on soybean (*Glycine max*) – rust (*Phakopsora pachyrhizi*) applied the BLINK method (Martins et al. 2022; Montejo Domínguez et al. 2022; Wu et al., 2022; Xiong et al. 2023). The number of significant marker-trait associated largely depended on the number and distribution of the available markers. Accordingly, 100 and 129 marker-trait associations were identified in response to rust in soybean and common bean in studies with more than 20,000 genome-wide markers (Wu et al. 2022; Xiong et al. 2023) while only 7 DS associated markers was identified in response to *U. pisi* in grass pea from a marker set of 5,651 SNPs (Martins et al. 2022). Interestingly, aligning these 7 grass pea markers onto pea reference genomes allowed the identification of 19 candidates genes among which 5 have similar function to those detected in the present study (Martins et al. 2022).

4.2 Candidate genes represent diverse functional roles

Examining the surrounding regions of the 95 associated markers detected in the present study allowed the identification of 62 candidate genes with potential function in rust resistance. According to their annotation, these candidate genes participate in a variety of function, including primary and secondary metabolism, cell wall synthesis, cell trafficking, DNA transcription regulation and defence response.

4.2.1 Regulators of gene expression

Among the 62 candidate genes, 12 are related to the regulation of DNA transcription/translation, RNA modification, and transposable elements. Seven of them are transcription factors (TFs), including a Nodule inception-like 9 protein (NLP9, 127087291) a Cycling DOF factor 3 (CDF3, 127105708) and a Zinc finger transcription factor orthologous to Tandem Zinc Finger 9 (TZF9, 127084564). Previous studies on TZF9 identified it as an important regulator of plant immune defence in *A. thaliana* (Maldonado-Bonilla et al. 2014; Tabassum et al. 2020). While NLP9 and CDF3 have been mainly associated with nitrogen use efficiency in plants some studies in tomato and soybean linked them to the response to biotic and abiotic stresses (Renau-Morata et al. 2017; Domínguez-Figueroa et al. 2020; Konishi et al. 2021; Amin et al. 2023). Interestingly, two candidate genes (127087323 and 127082537) encoding plant mobile domains are located within a 1.2Mb distance on both side of NPL9. While the role of these two genes in genomic regulation is under study, their involvement in plant defence has yet to be clarified (Fambrini et al. 2020). Apart from these TFs, two candidate genes (12782329 and 127126145), encoding a splicing factor (SF3b) of the U2 spliceosome complex and an RNA helicase (PRP22) respectively, are related to mRNA splicing via the spliceosome, which play an important role in the plant response to biotic stresses (Shang et al. 2017). Accordingly, knock-out mutation in SMD3, other subunits of the U2 complex, increase the susceptibility to *Pseudomonas syringae* in *A. thaliana* (Golisz et al. 2021). In addition, the orthologous gene of RNA helicase in *A. thaliana* (At1g32490) have been implicated in the negative regulation of numerous genes related to cell wall formation (Howles et al. 2016), which could improve the physical barrier against haustoria formation inside the plant cells.

4.2.2 Regulators of vesicle trafficking and cell wall components

Several of the candidate genes containing or closely related to the associated markers are related to vesicle trafficking and cell wall biosynthesis suggesting the importance of the cell wall and cell trafficking in response to rust. Among them, three genes (127087512, 127102730, and 127115771) encode proteins of the coat protein complex I (COPI), coat protein complex II (COPII), and clathrin-mediated endocytosis vesicles that mediate basic functions of protein export/import to the ER in plant cells (Zeng et al. 2023). COPII has been directly involved in the process of autophagy, which enable the ABA-mediated cell nutrient recycling in response to stress (Li et al. 2022). In addition, the gene 127086095 encodes an actin-related protein (ARP8) that participates in cytoskeleton-related functions (Kandasamy et al. 2008). Recent studies in *A. thaliana* have shown that related ARPs, such as ARP4 and ARP6, are involved in both

biotic and abiotic environmental changes (Nie and Wang 2021; Jakada et al. 2023). This suggest that vesicle trafficking, and particularly the endomembrane cell system, could play an important function in response to rust in pea.

On the other hand, eight candidate genes (127086095, 127076644, 127115471, 127137201, 127084018, 127082981, 127076644 and 127115471) are related to cell wall formation or to the biosynthesis of cell-wall related secondary metabolites such as lignin. Among them, gene 127137201 encodes a glycosyltransferase BC10 that have been related to the cellulose and lignin biosynthesis at the cell wall (Zhou et al. 2009; Zhang et al. 2016) while two genes (127082981 and 127084018) are related to the synthesis of rhamnogalacturonan-I (RG-I), one of the pectic components of the cell wall (Stonebloom et al. 2016). This suggests that changes in the cell wall composition may participate in the plant cell response to rust. Interestingly, two additional genes (127076644 and 127115471), encoded an Eceriferum (CER1) -like enzyme and a mid-chain alkane hydroxylase (MAH1), respectively, are important players of wax on the cell wall (Lewandowska et al. 2020; Wang et al. 2020) which play an important role in the host recognition by rust in several species (Niks and Rubiales 2002) and on the modulation of plant susceptibility to necrotrophic fungus such as *Sclerotinia sclerotiorum* (Bourdenx et al. 2011).

4.2.3 Regulators of hormone signaling and defense response

Eleven of the identified genes in the vicinity of the significantly associated markers were related to hormone signalling and defence. Among them, two genes (127080599 and 127125898) encoded two copies of a nodulin like proteins homologs to *Medicago truncatula* NODULIN 21 (MtN21) and *A. thaliana* WAT1 (walls are thin 1) genes that have been involved in auxin metabolism and play a significant role in secondary cell wall formation of (Ranocha et al. 2010). Recent studies showed that additional MtN21-related homologs in *A. thaliana*, such as RTP1 negatively regulates plant resistance to biotrophic pathogens through cell death and auxin-mediated production of reactive oxygen species (Pan et al. 2016; Gao et al. 2023) linking these genes to auxin signalling and defence. Apart for auxin, several genes pointed to the potential involvement of ABA in response to rust since four genes (127085672, 127091495, 127105022 and 127104606) encoded ABA-responsive genes including orthologs of the potassium channel AKT2/3, the regulatory subunit of protein phosphatase 1 (PP1R3), the Abscisic Acid Insensitive 4 (ABI4) and a SEC14-like protein (Chérel et al. 2002; Wang et al. 2016; Chandrasekaran et al. 2020; Zhang et al. 2020). Among their distinct functions, several studies in *A. thaliana* or *Nicotiana benthamiana* showed that AKT2/3, ABI4 and the SEC14 proteins contributed to plant defence being important actors of the plant resistance to different pathogens (Kiba et al. 2012; Zhou et al. 2014; Yop et al. 2023).

Several genes identified in this study are also directly involved in the plant defence mechanisms against pathogen attacks, involving some regulatory proteins and kinases. Accordingly, three of the identified genes encoded protein kinases including a PBS1-like protein kinase, a calcium-dependent protein kinase (CDPK3) and cysteine-rich receptor-like kinase (CRK8). Previous studies reported the crucial role of PBS1 in bacterial and viral resistance in *A. thaliana* and soybean (Pottinger et al. 2020). PBS1 was also shown to play a role in herbivore resistance in interaction with CDPK3 (Miyamoto et al. 2019; Desaki et al. 2023) hinting the involvement of both gene in a common defence pathway. Interestingly, one marker significantly associated with pea rust resistance was located at 8.27 kb of the receptor-like kinase CRK8 that have been shown previously to play a crucial role in rust resistance in wheat (Gu et al. 2020; Kamel et al. 2023). In addition to these kinases, this study identified an ortholog of a F-box protein CPR1/CPR30 (127117481), that acts, between other function, as a negative regulator of salicylic acid-dependent resistance (R) proteins like SNC1 (Gou et al. 2012), and a dynamin-related protein 1E (DRP1E; 127127894) which knock-out mutation was found in *A. thaliana* to induce stronger hypersensitive response to powdery mildew (Tang et al. 2006; Leibman-Markus et al. 2022; Mc Gowan et al. 2022).

Altogether, this GWAS study shed light on the complex genetic architecture underpinning partial resistance to rust in pea. In addition to the detection of 95 new molecular markers associated with partial resistance, this study detected 62 candidate genes that contains or was intricately linked to these markers, which offer several promising targets to improve our understanding of rust resistance in pea and future plant breeding strategies. These genes span a diverse array of biological functions providing the basis for further gene functional mapping. The identification of several candidate genes known to participate in rust resistance in cereal (i.e., wax genes, CRK8) suggest that at least some of these candidate genes might be the responsible gene underlying the detected QTL confirming the usefulness of GWAS

studies to uncover new resistance QTL and genes. Therefore, this study opens the possibility to characterize further, via gene expression studies or TILLING, the function of these candidate genes to explore their implication in rust disease in pea. The significantly associated DArT-seq markers also provides a basis for future marker-assisted selection and the development of more efficient genomic prediction models for rust resistance. Therefore, this study contributes to understanding the genetic make-up of rust resistance in pea and promotes future crop improvement. By focusing on the candidate genes uncovered, breeding programs can develop more targeted approaches, upon their validation, leveraging genetic variation to improve the resilience of pea crops against rust disease. These findings open new avenues for precision breeding, offering novel targets for rust resistance improvement and enhancement of crop resilience and productivity through the development of new pea rust-resistant varieties. This not only contributes to secure yield and quality in the face of biotic stress but also supports sustainable agricultural practices by reducing the reliance on chemical fungicides.

5 Data availability

The DArTseq marker datasets analysed during the current study are available in the Zenodo repository, https://zenodo.org/records/7180467. The phenotypic datasets generated and analysed are available in the GitHub repository, https://github.com/SalvaOsuna/Rust-collection.git.

6 References

Adhikari KN, Khazaei H, Ghaouti L, Maalouf F, Vandenberg A, Link W et al (2021) Conventional and Molecular Breeding Tools for Accelerating Genetic Gain in Faba Bean (*Vicia faba* L.). Front Plant Sci 12:1–17. https://doi.org/10.3389/fpls.2021.744259

Alemu A, Brantestam AK, Chawade A (2022) Unraveling the Genetic Basis of Key Agronomic Traits of Wrinkled Vining Pea (*Pisum sativum* L.) for Sustainable Production. Front Plant Sci 13. https://doi.org/10.3389/fpls.2022.844450

Amin N, Ahmad N, Khalifa MAS, Du Y, Mandozai A, Khattak AN et al (2023) Identification and Molecular Characterization of RWP-RK Transcription Factors in Soybean. Genes (Basel) 14:369. https://doi.org/10.3390/genes14020369

Astle W, Balding DJ (2009) Population Structure and Cryptic Relatedness in Genetic Association Studies. Stat Sci 24. https://doi.org/10.1214/09-STS307

Avila CM, Sillero JC. Rubiales D, Moreno MT, Torres AM (2003) Identification of RAPD markers linked to the Uvf-1 gene conferring hypersensitive resistance against rust (*Uromyces viciae-fabae*) in *Vicia faba* L. Theor Appl Genet 107:353–358. https://doi.org/10.1007/s00122-003-1254-8

Barilli E, Agudo FJ, Masi M, Nocera P, Evidente A, Rubiales D (2022) Anthraquinones and their analogues as potential biocontrol agents of rust and powdery mildew diseases of field crops. Pest Manag Sci 78:3489–3497. https://doi.org/10.1002/ps.6989

Barilli E, Cimmino A, Masi M, Evidente M, Rubiales D, Evidente A (2017) Inhibition of early development stages of rust fungi by the two fungal metabolites cyclopaldic acid and epi-epoformin. Pest Manag Sci 73:1161–1168. https://doi.org/10.1002/ps.4438

Barilli E, Cobos MJ, Carrillo E, Kilian A, Carling J, Rubiales D (2018) A high-density integrated DArTseq SNP-based genetic map of *Pisum fulvum* and identification of QTLs controlling rust resistance. Front Plant Sci 9:1–13. https://doi.org/10.3389/fpls.2018.00167

Barilli E, Moral A, Sillero JC, Rubiales D (2012a) Clarification on rust species potentially infecting pea (*Pisum sativum* L.) crop and host range of *Uromyces pisi* (Pers.) Wint. Crop Prot 37:65–70. https://doi.org/10.1016/j.cropro.2012.01.019

Barilli E, Rubiales D, Castillejo MA (2012b) Comparative proteomic analysis of BTH and BABA-induced resistance in pea (*Pisum sativum*) toward infection with pea rust (*Uromyces pisi*). J Proteomics 75:5189–5205. https://doi.org/10.1016/j.jprot.2012.06.033

Barilli E, Sillero JC, Fernández-Aparicio M, Rubiales D (2009a) Identification of resistance to *Uromyces pisi* (Pers.) Wint. in *Pisum* spp. germplasm. F Crop Res 114:198–203. https://doi.org/10.1016/j.fcr.2009.07.017

Barilli E, Sillero JC, Prats E, Rubiales D (2014) Resistance to rusts (*Uromyces pisi* and *U. viciae-fabae*) in pea. Czech J Genet Plant Breed 50:135–143. https://doi.org/10.17221/125/2013-cjgpb

Barilli E, Sillero JC, Rubiales D (2009b). Induction of Systemic Acquired Resistance in Pea against Rust (*Uromyces pisi*) by Exogenous Application of Biotic and Abiotic Inducers. J Phytopathol 158:30-34. https://doi.org/10.1111/j.1439-0434.2009.01571.x

Bates D, Mächler M, Bolker BM, Walker SC (2015) Fitting linear mixed-effects models using lme4. J Stat Softw 67. https://doi.org/10.18637/jss.v067.i01

Bourdenx B, Bernard A, Domergue F, Pascal S, Léger A, Roby D et al (2011) Overexpression of Arabidopsis ECERIFERUM1 Promotes Wax Very-Long-Chain Alkane Biosynthesis and Influences Plant Response to Biotic and Abiotic Stresses. Plant Physiol 156:29–45. https://doi.org/10.1104/pp.111.172320

Chandrasekaran U, Luo X, Zhou W, Shu K (2020) Multifaceted Signaling Networks Mediated by Abscisic Acid Insensitive 4. Plant Commun 1:100040. https://doi.org/10.1016/j.xplc.2020.100040

Chérel I, Michard E, Platet N, Mouline K, Alcon C, Sentenac H et al (2002) Physical and Functional Interaction of the Arabidopsis K + Channel AKT2 and Phosphatase AtPP2CA. Plant Cell 14:1133–1146. https://doi.org/10.1105/tpc.000943

Clemente A, Olias R (2017) Beneficial effects of legumes in gut health. Curr Opin Food Sci 14:32–36. https://doi.org/10.1016/j.cofs.2017.01.005

Desaki Y, Morishima M, Sano Y, Uemura T, Ito A, Nemoto K et al (2023) Cytoplasmic Kinase Network Mediates Defense Response to *Spodoptera litura* in Arabidopsis. Plants 12:1747. https://doi.org/10.3390/plants12091747

Emeran AA, Sillero JC, Fernández-Aparicio M, Rubiales D (2011) Chemical control of faba bean rust (*Uromyces viciae-fabae*). Crop Prot 30:907-912. https://doi.org/10.1016/j.cropro.2011.02.004

Fambrini M, Usai G, Vangelisti A, Mascagni F, Pugliesi C (2020) The plastic genome: The impact of transposable elements on gene functionality and genomic structural variations. genesis 58. https://doi.org/10.1002/dvg.23399

FAOSTAT (2021) Statistics Division of the Food and Agriculture Organization of the United Nations. http://www.fao.org/faostat/en/#data/QC. (01–06–2023)

Gallego-Sánchez LM, Canales FJ, Montilla-Bascón G, Prats E (2020) RUST: A Robust, User-Friendly Script Tool for Rapid Measurement of Rust Disease on Cereal Leaves. Plants 9:1182. https://doi.org/10.3390/plants9091182

Gao X, Tang Y, Shi Q, Wei Y, Wang X, Shan W et al (2023) Vacuolar processing enzyme positively modulates plant resistance and cell death in response to *Phytophthora parasitica* infection. J Integr Agric 22:1424–1433. https://doi.org/10.1016/j.jia.2022.08.124

Golisz A, Krzyszton M, Stepien M, Dolata J, Piotrowska J, Szweykowska-Kulinska Z et al (2021) Arabidopsis Spliceosome Factor SmD3 Modulates Immunity to *Pseudomonas syringae* Infection. Front Plant Sci 12. https://doi.org/10.3389/fpls.2021.765003

Gou M, Shi Z, Zhu Y, Bao Z, Wang G, Hua J (2012) The F□box protein CPR1/CPR30 negatively regulates R protein SNC1 accumulation. Plant J 69:411–420. https://doi.org/10.1111/j.1365-313X.2011.04799.x

Gu J, Sun J, Liu N, Sun X, Liu C, Wu L et al (2020) A novel cysteine□rich receptor□like kinase gene, TaCRK2, contributes to leaf rust resistance in wheat. Mol Plant Pathol 21:732–746. https://doi.org/10.1111/mpp.12929

Gungaabayar A, Jha A, Warkentin T, Knight D, Penner G, Biligetu B (2023) Forage yield and biological nitrogen fixation of pea–cereal intercrops for hay production. Agron J 115:607–619. https://doi.org/10.1002/agj2.21270

Howles PA, Gebbie LK, Collings DA, Varsani A, Broad RC, Ohms S et al (2016) A temperature-sensitive allele of a putative mRNA splicing helicase down-regulates many cell wall genes and causes radial swelling in *Arabidopsis thaliana*. Plant Mol Biol 91:1–13. https://doi.org/10.1007/s11103-016-0428-0

Huang M, Liu X, Zhou Y, Summers RM, Zhang Z (2019) BLINK: A package for the next level of genome-wide association studies with both individuals and markers in the millions. Gigascience 8:1–12. https://doi.org/10.1093/gigascience/giy154

Jakada BH, Fakher B, Yao L-A, Wang X, Aslam M, Qin Y (2023) Ectopic Expression of Pineapple Actin-Related Protein 6 (AcARP6) Regulates Flowering and Stress Responses in Arabidopsis. J Plant Growth Regul 42:6461–6473. https://doi.org/10.1007/s00344-022-10874-0

Kamel AM, Metwally K, Sabry M, Albalawi DA, Abbas ZK, Darwish DBE et al (2023) The Expression of *Triticum aestivum* Cysteine-Rich Receptor-like Protein Kinase Genes during Leaf Rust Fungal Infection. Plants 12:2932. https://doi.org/10.3390/plants12162932

Kandasamy MK, McKinney EC, Meagher RB. (2008) ACTIN-RELATED PROTEIN8 Encodes an F-Box Protein Localized to the Nucleolus in Arabidopsis. Plant Cell Physiol 49:858–863. https://doi.org/10.1093/pcp/pcn053

Kassambara A, Mundt F (2020) factoextra: Extract and Visualize the Results of Multivariate Data Analyses. R Packag. version 1.0.7. https://cran.r-project.org/package=factoextra

Kaur G, Toora PK, Tuan PA, McCartney CA, Izydorczyk MS, Badea A et al (2023) Genome-wide association and targeted transcriptomic analyses reveal loci and candidate genes regulating preharvest sprouting in barley. Theor Appl Genet 136:202. https://doi.org/10.1007/s00122-023-04449-0

Kiba A, Nakano M, Vincent-Pope P, Takahashi H, Sawasaki T, Endo Y et al (2012) A novel Sec14 phospholipid transfer protein from *Nicotiana benthamiana* is up-regulated in response to *Ralstonia solanacearum* infection, pathogen associated molecular patterns and effector molecules and involved in plant immunity. J Plant Physiol 169:1017–1022. https://doi.org/10.1016/j.jplph.2012.04.002

Kreplak J, Madoui MA, Cápal P, Novák P, Labadie K, Aubert G et al (2019) A reference genome for pea provides insight into legume genome evolution. Nat Genet 51:1411–1422. https://doi.org/10.1038/s41588-019-0480-1

Leprévost T, Boutet G, Lesné A, Rivière J-P, Vetel P, Glory I et al (2023) Advanced backcross QTL analysis and comparative mapping with RIL QTL studies and GWAS provide an overview of QTL and marker haplotype diversity for resistance to Aphanomyces root rot in pea (*Pisum sativum*). Front Plant Sci 14. https://doi.org/10.3389/fpls.2023.1189289.

Lewandowska M, Keyl A, Feussner I (2020) Wax biosynthesis in response to danger: its regulation upon abiotic and biotic stress. New Phytol 227:698–713. https://doi.org/10.1111/nph.16571

Li B, Zeng Y, Jiang L (2022) COPII vesicles in plant autophagy and endomembrane trafficking. FEBS Lett 596:2314–2323. https://doi.org/10.1002/1873-3468.14362

Lilin-Yin (2023) CMplot: Circle Manhattan Plot. CRAN. https://cran.r-project.org/package=CMplot

Maldonado-Bonilla LD, Eschen-Lippold L, Gago-Zachert S, Tabassum N, Bauer N, Scheel D et al (2014). The Arabidopsis Tandem Zinc Finger 9 Protein Binds RNA and Mediates Pathogen-Associated Molecular Pattern-Triggered Immune Responses. Plant Cell Physiol 55:412–425. https://doi.org/10.1093/pcp/pct175

Martins DC, Rubiales D, Vaz Patto MC (2022) Association Mapping of *Lathyrus sativus* Disease Response to *Uromyces pisi* Reveals Novel Loci Underlying Partial Resistance. Front Plant Sci 13. https://doi.org/10.3389/fpls.2022.842545

Miyamoto T, Uemura T, Nemoto K, Daito M, Nozawa A, Sawasaki T et al (2019) Tyrosine Kinase-Dependent Defense Responses Against Herbivory in Arabidopsis. Front Plant Sci 10. https://doi.org/10.3389/fpls.2019.00776

Montejo Domínguez L de MA, McClean PE, Steadman J, McCoy S, Markell S, Osorno JM (2022) Bean rust resistance in the Guatemalan climbing bean germplasm collection. Legum Sci 4. https://doi.org/10.1002/leg3.149

Negussie TG, Bender CM, Van Wyk PWJ Pretorius ZA (2012). Hypersensitivity of rust resistance in lentil. South African J Plant Soil 29:25–29. https://doi.org/10.1080/02571862.2012.688377

Niks RE and Rubiales D (2002) Potentially durable resistance mechanisms in plants to specialised fungal pathogens. Euphytica 124:201–216. https://doi.org/10.1023/A:1015634617334

Olivoto T, Andrade SMP, Del Ponte E (2022) Measuring plant disease severity in R: introducing and evaluating the pliman package. Trop Plant Pathol 47:95–104. https://doi.org/10.1007/s40858-021-00487-5

Olivoto T, Lúcio AD (2020) metan: an R package for multi-environment trial analysis. Methods Ecol Evol 11:783-789. https://doi.org/10.1111/2041-210X.13384

Osuna-Caballero S, Olivoto T, Jiménez-Vaquero MA, Rubiales D, Rispail N (2023) RGB image-based method for phenotyping rust disease progress in pea leaves using R. Plant Methods 19:86. https://doi.org/10.1186/s13007-023-01069-z

Osuna-Caballero S, Rispail N, Barilli E, Rubiales D (2022) Identification and Characterization of Novel Sources of Resistance to Rust Caused by *Uromyces pisi* in *Pisum* spp. Plants 11:2268. https://doi.org/10.3390/plants11172268

Pan Q, Cui B, Deng F, Quan J, Loake GJ, Shan W (2016) RTP 1 encodes a novel endoplasmic reticulum (ER)□localized protein in Arabidopsis and negatively regulates resistance against biotrophic pathogens. New Phytol 209:1641–1654. https://doi.org/10.1111/nph.13707.

Petrovski S, Wang Q (2016) QQperm: Permutation Based QQ Plot and Inflation Factor Estimation. R Packag. version 1.0.1. https://cran.r-project.org/package=QQperm

Pottinger SE, Bak A, Margets A, Helm M, Tang L, Casteel C et al (2020) Optimizing the PBS1 Decoy System to Confer Resistance to Potyvirus Infection in Arabidopsis and Soybean. Mol Plant-Microbe Interact 33:932–944. https://doi.org/10.1094/MPMI-07-19-0190-R

R Core Team (2021). R: A Language and Environment for Statistical Computing. R Found. Stat Comput Vienna. https://www.r-project.org/.

Ranocha P, Denancé N, Vanholme R, Freydier A, Martinez Y, Hoffmann L et al (2010) Walls are thin 1 (WAT1), an Arabidopsis homolog of *Medicago truncatula* NODULIN21, is a tonoplast-localized protein required for secondary wall formation in fibers. Plant J 63:469–483. https://doi.org/10.1111/j.1365-313X.2010.04256.x

Renau-Morata B, Molina RV, Carrillo L, Cebolla-Cornejo J, Sánchez-Perales M, Pollmann S et al (2017) Ectopic Expression of CDF3 Genes in Tomato Enhances Biomass Production and Yield under Salinity Stress Conditions. Front Plant Sci 8. https://doi.org/10.3389/fpls.2017.00660

Rispail N, Wohor OZ, Osuna-Caballero S, Barilli E, Rubiales D (2023) Genetic Diversity and Population Structure of a Wide *Pisum* spp. Core Collection. Int J Mol Sci 24:2470. https://doi.org/10.3390/ijms24032470

Rubiales D, Barilli E, Rispail N (2023) Breeding for Biotic Stress Resistance in Pea. Agriculture 13:1825. https://doi.org/10.3390/agriculture13091825

Rubiales D, Castillejo MA, Madrid E, Barilli E, Rispail N (2011) Legume breeding for rust resistance: lessons to learn from the model *Medicago truncatula*. Euphytica 180:89-98. https://doi.org/10.1007/s10681-011-0367-4

Rubiales D, Fondevilla S, Chen W, Gentzbittel L, Higgins TJV, Castillejo MA et al (2015) Achievements and Challenges in Legume Breeding for Pest and Disease Resistance. CRC Crit Rev Plant Sci 34:195–236. https://doi.org/10.1080/07352689.2014.898445

Rubiales D, González-Bernal MJ, Warkentin T, Bueckert R, Vaz Patto MC, McPhee K, McGee R, Smýkal P (2019) CH20 - Advances in breeding of peas. In: Hochmuth G (Ed), Achieving sustainable cultivation of vegetables, Burleig Dodds Science Publishing Limited, Cambridge, UK, http://dx.doi.org/10.19103/AS.2019.0045.28

Rubiales D, Rojas-Molina MM, Sillero JC (2013) Identification of pre- and posthaustorial resistance to rust (*Uromyces viciae-fabae*) in lentil (*Lens culinaris*) germplasm. Plant Breed 132:676–680. https://doi.org/10.1111/pbr.12096

Shang X, Cao Y, Ma L (2017) Alternative Splicing in Plant Genes: A Means of Regulating the Environmental Fitness of Plants. Int J Mol Sci 18:432. https://doi.org/10.3390/ijms18020432

Singh AK, Kushwaha C, Shikha K, Chand R, Mishra GP, Dikshit HK et al (2023) Rust (*Uromyces viciae-fabae* Pers. de-Bary) of Pea (*Pisum sativum* L.): Present Status and Future Resistance Breeding Opportunities. Genes (Basel) 14:374. https://doi.org/10.3390/genes14020374

Skoufogianni E, Giannoulis K, Bartzialis D, Danalatos N (2019) Relations between crop rotation with pea and soil structure. Bulg J Agric Sci 25 1205–1210

Stonebloom S, Ebert B, Xiong G, Pattathil S, Birdseye D, Lao J et al (2016) A DUF-246 family glycosyltransferase-like gene affects male fertility and the biosynthesis of pectic arabinogalactans. BMC Plant Biol 16:90. https://doi.org/10.1186/s12870-016-0780-x

Storey JD Tibshirani R (2003) Statistical significance for genomewide studies. Proc Natl Acad Sci USA 100:9440–9445. https://doi.org/10.1073/pnas.1530509100

Storey JD, Bass AJ (2022) qvalue: Q-value estimation for false discovery rate control. R Packag. version 2.30.0. http://github.com/jdstorey/qvalue

Susmitha P, Kumar P, Yadav P, Sahoo S, Kaur G, Pandey MK et al (2023) Genome-wide association study as a powerful tool for dissecting competitive traits in legumes. Front Plant Sci 14. https://doi.org/10.3389/fpls.2023.1123631

Tabassum N, Eschen□Lippold L, Athmer B, Baruah M, Brode M, Maldonado□Bonilla LD et al (2020) Phosphorylation□dependent control of an RNA granule□localized protein that fine□tunes defence gene expression at a post□transcriptional level. Plant J 101:1023–1039. https://doi.org/10.1111/tpj.14573

Tang D, Ade J, Frye CA, Innes RW (2006) A mutation in the GTP hydrolysis site of Arabidopsis dynamin□related protein 1E confers enhanced cell death in response to powdery mildew infection. Plant J 47:75–84. https://doi.org/10.1111/j.1365-313X.2006.02769.x

Tibbs Cortes L, Zhang Z, Yu J (2021) Status and prospects of genome□wide association studies in plants. Plant Genome 14. https://doi.org/10.1002/tpg2.20077

Tulbek MC, Lam RSH, Wang YC, Asavajaru P, Lam A (2016) Pea: A Sustainable Vegetable Protein Crop. Elsevier Inc. https://doi.org/10.1016/B978-0-12-802778-3.00009-3

Wang J, Wang Y, Liu X, Xu Y, Ma Q (2016) Microtubule Polymerization Functions in Hypersensitive Response and Accumulation of H2O2 in Wheat Induced by the Stripe Rust. Biomed Res Int 2016. https://doi.org/10.1155/2016/7830768

Wang J, Zhang Z (2021) GAPIT Version 3: Boosting Power and Accuracy for Genomic Association and Prediction. Genomics Proteomics Bioinformatics 19:629–640. https://doi.org/10.1016/j.gpb.2021.08.005

Wu X, Wang B, Xin Y, Wang Y, Tian S, Wang J et al (2022) Unravelling the Genetic Architecture of Rust Resistance in the Common Bean (*Phaseolus vulgaris* L.) by Combining QTL-Seq and GWAS Analysis. Plants 11:953. https://doi.org/10.3390/plants11070953.

Xiong H, Chen Y, Pan Y-B, Wang J, Lu W, Shi A (2023) A genome-wide association study and genomic prediction for *Phakopsora pachyrhizi* resistance in soybean. Front Plant Sci 14. https://doi.org/10.3389/fpls.2023.1179357

Yang T, Liu R, Luo Y, Hu S, Wang D, Wang C et al (2022) Improved pea reference genome and pan-genome highlight genomic features and evolutionary characteristics. Nat Genet 54:1553–1563. https://doi.org/10.1038/s41588-022-01172-2

Yop GS, Gair LHV, da Silva VS, Machado ACZ, Santiago DC, Tomaz JP (2023) Abscisic Acid Is Involved in the Resistance Response of *Arabidopsis thaliana* Against *Meloidogyne paranaensis*. Plant Dis 107:2778–2783. https://doi.org/10.1094/PDIS-07-22-1726-RE

Zeng Y, Liang Z, Liu Z, Li B, Cui Y, Gao C et al (2023) Recent advances in plant endomembrane research and new microscopical techniques. New Phytol 240:41–60. https://doi.org/10.1111/nph.19134

Zhang J, Qin Q, Nan X, Guo Z, Liu Y, Jadoon S et al (2020) Role of Protein Phosphatase1 Regulatory Subunit3 in Mediating the Abscisic Acid Response. Plant Physiol 184:1317–1332. https://doi.org/10.1104/pp.20.01018

Zhou L, He H, Liu R, Han Q, Shou H, Liu B (2014) Overexpression of GmAKT2potassium channel enhances resistance to soybean mosaic virus. BMC Plant Biol 14:154. https://doi.org/10.1186/1471-2229-14-154

Zhou Y, Li S, Qian Q, Zeng D, Zhang M, Guo L et al (2009) BC10, a DUF266□containing and Golgi□located type II membrane protein, is required for cell□wall biosynthesis in rice (*Oryza sativa* L.). Plant J 57:446–462. https://doi.org/10.1111/j.1365-313X.2008.03703.x

7 Acknowledgements

The authors acknowledge Manuel A. Jiménez-Vaquero for assisting with the pea evaluations under controlled condition with the rust UpKeS-05 isolate.

8 Funding

This research was supported by the projects PID2020-114668RB-100, PDC2021-120930-I00 and PRE2018-083717 funded by MCIN/AEI/10.13039/501100011033.

9 Author Contribution Statement

DR and NR conceived the original idea for this study. SOC conducted the experiments and took the lead in manuscript writing. SOC analysed the data with help from NR. SOC designed the figures and tables with input from NR and DR, who also significantly contributed to data interpretation and provided critical feedback that shaped the final version of the manuscript. DR acquired the funding for this project. All authors approved the submitted version.

10 Conflict of interest

The authors declare that they have no conflict of interest.

11 Ethics approval

All experiments described in this manuscript comply with the current laws of the country in which they were performed.